

COMPARISON OF AEROSOL MICROPHYSICAL PARAMETERS RETRIEVED FROM MULTI-WAVELENGTH LIDAR AND SUN PHOTOMETER

I. Veselovskii⁽¹⁾, D.N. Whiteman⁽²⁾, O.Dubovik⁽³⁾, A. Kolgotin⁽¹⁾, M.Korenskii⁽¹⁾

⁽¹⁾Physics Instrumentation Center, Troitsk, Moscow Region, 142190, Russia, E-mail: igorv@quadra.ru

⁽²⁾NASA GSFC, Greenbelt MD 20771, USA, E-mail: david.n.whiteman@nasa.gov

⁽³⁾NASA GSFC, Greenbelt MD 20771, USA, E-mail: dubovik@eronet.gsfc.nasa.gov

ABSTRACT

Multiwavelength lidars are a promising tool for profiling tropospheric aerosol microphysical parameters. To study this technique further the lidar derived parameters are compared with column-integrated aerosol properties provided by the robotic sun photometer that is used in the network called AERONET. In our report we present results obtained with a multi-wavelength Raman lidar developed at NASA/GSFC. This lidar is used to quantify three aerosol backscattering and two extinction coefficients. Aerosol microphysical parameters are retrieved from these optical data by using inversion with regularization. Vertical profiles of volume concentration, effective radius and complex refractive index are compared with column-integrated values measured by sun photometer. The results demonstrate that the lidar-derived values are in good agreement with the more established sun photometer results. Comparison of particles size distribution shows that the lidar reproduces the fine mode well, but has difficulty retrieving the coarse mode with similar accuracy.

1. INTRODUCTION

Lidar profiling of tropospheric aerosols is a rapidly developing research field. Numerous theoretical and experimental studies performed during the last decade have demonstrated that the multi-wavelength lidar technique is able to provide comprehensive information about aerosol microphysical parameters. The results thus established demonstrate that the key to successful retrieval of aerosol parameters is the joint use of aerosol backscattering and extinction coefficients^{1,2}, which dictates the use of Raman or high spectral resolution lidars. Another important finding is that a simplified multi-wavelength Raman lidar that is based on a frequency-tripled Nd:YAG laser allows estimation of the particle size distribution (PSD) and complex refractive index³.

To study this technique further the lidar-derived parameters can be compared with comparable results from other instruments. One of the recognized

instruments for retrieval of column-integrated aerosol properties is the robotic sun photometer (SP) that is used in the network called AERONET^{4,5}. The comparison of lidar and sun photometer data has been performed in several publications^{6,7}. In these studies the comparisons were limited mainly to aerosol optical density, Angstrom parameter and lidar ratios. To our knowledge, the only comparison of particle microphysical parameters derived from both instruments was reported in recent publication of Muller et. al⁸. That comparison demonstrates reasonable agreement between lidar and sun photometer. Still, to prove the potential of multi-wavelength lidar technique, additional comparisons and detailed analysis of obtained data are needed.

In our report we present the results of lidar measurements in the summer of 2005 at Greenbelt, MD. We should mention also that our final goal is the use of sun photometer data as a constraint in multi-wavelength lidar inversion algorithm, so the comparisons presented here constitute a first step toward this goal.

2. SYSTEM DESCRIPTION

The experiments were performed with a multi-wavelength Raman lidar developed at NASA/GSFC. The lidar is based on a tripled Nd:YAG laser with 50 Hz repetition rate. The output powers at 355, 532 and 1064 nm are 20, 7.5 and 14 W respectively. The backscattered light is collected by a 40-cm aperture Schmidt-Cassegrain telescope with operational field of view of 0.35 mrad. The telescope is connected through an optical fiber to a receiving module that includes an off-axis parabolic mirror for collimation. The spectral components of the collimated signal are separated by dichroic mirrors and interference filters and detected using photomultiplier tubes or APDs (Hamamatsu R1924 PMTs, H7422P-40 module (607 nm), Licel IR enhanced Si APD in analog mode (1064 nm). In the current configuration of the system we are able to detect three elastic backscatters and two nitrogen Raman signals at 387 and 607 nm. The detection

system also has provisions to measurement both vapor and liquid water although those data are not analyzed here. Recording of both Raman and backscatter signals allows independent calculation of the particle backscattering β and extinction α coefficients. Our previous studies³ demonstrate that quantifying these three aerosol backscattering β and two extinction α coefficients is sufficient for estimation of aerosol microphysical parameters.

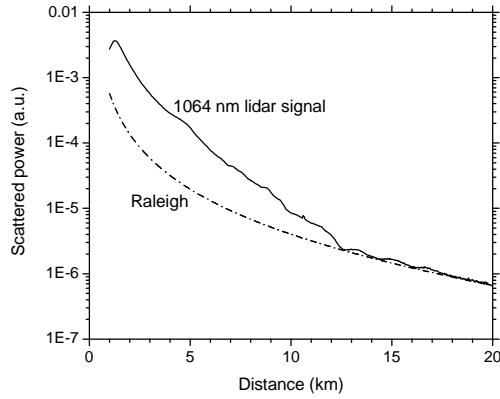


Fig.1. Lidar signal at 1064 nm measured on 2 August, 2005 together with simulated Raleigh backscattering (dash-dot).

The measurements were performed during July-August 2005 period. This season in the vicinity of Washington, DC is frequently characterized by hazy conditions and provides excellent opportunity for comparison with sun photometer. The majority of aerosols are concentrated inside planetary boundary layer (PBL). Particles are close to spherical and their parameters don't vary strongly through PBL. In particles size distribution fine mode is dominating, which is also convenient, because retrieval of coarse mode from the multi-wavelength lidar measurements is more difficult at a present time.

For comparison with sun photometer it is desirable to perform the measurements starting from as low altitudes as possible. To accomplish this we performed the measurements with the lidar system operating at 18 degrees above the horizon. No special correction for overlap function was made, so finally backscattering and extinction coefficients were calculated starting from 0.75 km altitude. Measurements were performed in nighttime (about 9 pm of local time) to detect Raman signals at sufficient height. This was 2 hours later than last sun photometer measurement.

Lidar signals at wavelength λ originated from Rayleigh-Mie P_λ and Raman P_R scattering are described by equations:

$$P_\lambda(z) = A_\lambda \frac{1}{z^2} [\beta_\lambda^m(z) + \beta_\lambda^a(z)] \exp \left[-2 \int_0^z (\alpha_\lambda^m(z) + \alpha_\lambda^a(z)) dz \right]$$

$$P_{\lambda_R}(z) = A_{\lambda_R} \frac{1}{z^2} \beta_R(z) \exp \left[- \int_0^z (\alpha_\lambda^m(z) + \alpha_\lambda^a(z) + \alpha_{\lambda_R}^m(z) + \alpha_{\lambda_R}^a(z)) dz \right]$$

Where A_λ is range independent parameter; β_λ^m , β_λ^a , α_λ^m , α_λ^a are molecular and aerosol backscattering and extinction coefficients, β_R is Raman nitrogen backscattering. For $\lambda=355$ and 532 nm these equations allow independent calculation of aerosol extinction and backscattering coefficients.

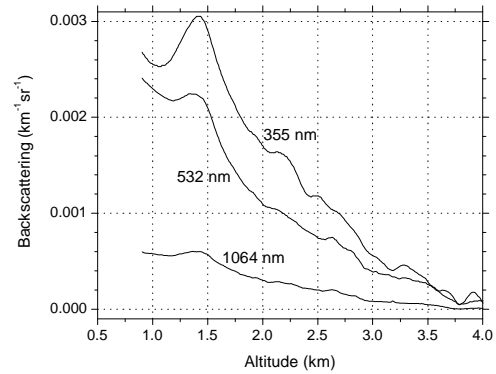


Fig.2. Vertical profiles of backscattering coefficients measured on 2 August 2005.

One of the most serious problems in data processing is the calculation of the backscattering coefficient at 1064 nm. In our algorithm for the computation of β_{1064} we choose the reference distance z_{ref} where Raleigh scattering is dominated and aerosol contribution is negligible. Fig.1 shows that such situation is realized for $z_{ref} > 14$ km. It is interesting to note that the molecular signal is more easily observed at 1064 with measurements at a low angle with respect to the horizon as done here. Calculation of β_{1064} is performed from equation for elastic scattering, where extinction profile is taken from 532 nm measurements and extrapolated to 1064 nm through

relationship $\frac{\alpha_{\lambda_2}^a}{\alpha_{\lambda_1}^a} = \left(\frac{\lambda_2}{\lambda_1} \right)^k$. Here k is Angstrom

parameter, calculated from $\frac{\alpha_{355}}{\alpha_{532}}$ ratio. The Angstrom parameter from AERONET has been used for this extrapolation.

3. RESULTS OF THE MEASUREMENTS

Fig.2 shows the vertical profiles of backscattering and extinction coefficients measured on 2 August, 2005. Here and further the vertical profiles are shown as a function of altitude H calculated as $H = z \cdot \sin \varphi$ where φ

is the angle of sounding. These data were used as input to retrieve aerosol microphysical parameters through inversion with regularization. With our algorithm described in Ref.2 we retrieve effective radius (r_{eff}), particle number (N_i), surface (S_i), volume (V_i) densities, and also real m_R and imaginary m_I part of refractive index. As shown previously, the results of the retrieval depend on the type of kernels used. The optimal results are attained when retrieval is performed with both number and volume kernels and the average of obtained values is taken.

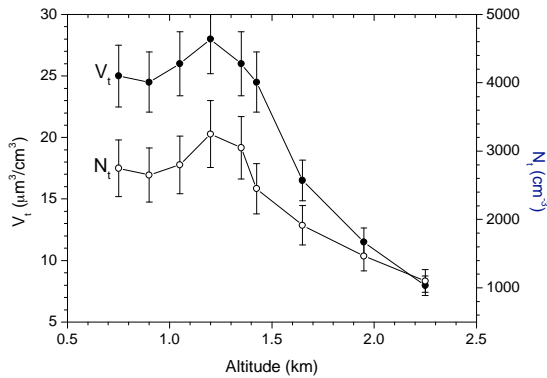


Fig.3. Vertical profile of volume (V_i) and number density (N_i) concentration on 2 August, 2005

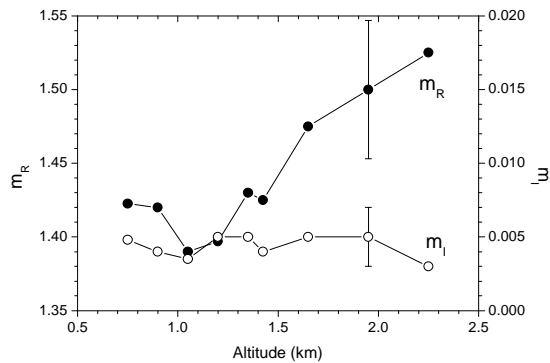


Fig.4. Vertical profile of real and imaginary part of refractive index on 2 August, 2005

The vertical profiles of number and volume densities are shown in Fig.3, both S_i and V_i have peaks at $H \approx 1.2$ km. Fig.4 shows the vertical variation of m_R and m_I . The uncertainty of refractive index retrieval is ± 0.05 for the real part and about 50% for imaginary part. Still we can conclude that m_R rises with altitude, while m_I stays constant (within the uncertainty). In SP measurements the real part rises from 1.37 to 1.4 in 450-1000 nm spectral range. The imaginary part is around 0.0044 and its spectral variation is insignificant. To compare these two instruments we have calculated from lidar data the weighted value of m_R

$$\text{as } \frac{\int V_i(H) m_R(H) dH}{\int V_i(H) dH}. \text{ Extrapolating } V(H) \text{ and } m_R(H)$$

below 0.75 km as a constant the weighted value of m_R is 1.42. The uncertainty of m_R retrieval from sun photometer is also about ± 0.05 so the obtained values are in a reasonable agreement. The imaginary part from the lidar measurements is of 0.005 ± 0.0025 , so it is also in agreement with sun photometer.

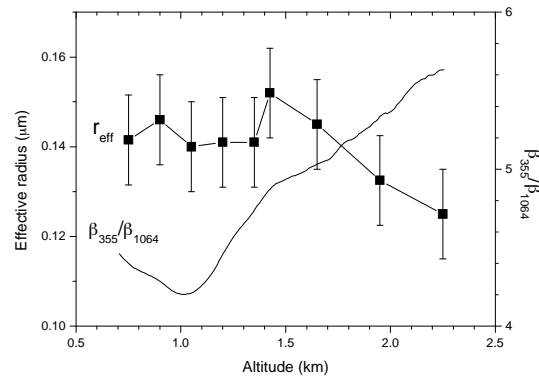


Fig.5. Altitude profiles of retrieved particles effective radius and color ratio $\frac{\beta_{355}}{\beta_{1064}}$ on 2 August, 2005

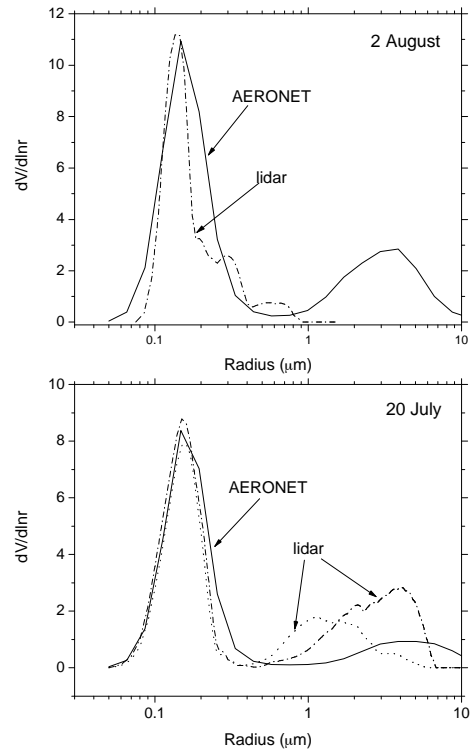


Fig.6. Comparison of particles size distribution retrieved from sun photometer and lidar on 2 August and 20 July 2005.

Another important parameter for comparison is height integrated volume concentration. Lidar measurements brings us to the value (for fine mode) $C_v=55\pm 10 \mu\text{m}^3/\text{cm}^2$ while sun photometer gives $75 \mu\text{m}^3/\text{cm}^2$. The obtained values agree reasonably well, because we had to extrapolate the profile $V_t(H)$ to the ground level, while concentration is usually increased toward the ground.

The effective radius of the fine mode derived from lidar measurements is about $0.14\pm 0.1 \mu\text{m}$, and it decreases to $0.12 \mu\text{m}$ for altitudes above 1.5 km, as it is shown in Fig.5. The sun photometer gives a value of $0.15 \mu\text{m}$ for the fine mode. The decrease of particle size for $H>1.5 \text{ km}$ is accompanied by the rise of the

ratio $\frac{\beta_{355}}{\beta_{1064}}$, which is physically understandable (recall

that this ratio is about 1 for big particles and about $\left(\frac{1064}{355}\right)^4$ for particles with radii $r\ll\lambda$).

Fig.6 shows comparison of PSD retrieved from sun photometer and lidar. In all our measurements fine mode is reproduced quite well, but often we failed to retrieve coarse mode with acceptable accuracy. The lidar derived PSD on 2 August, 2005 is shown for the middle of the PBL at $H=1.2 \text{ km}$. The PSDs are quite similar through the PBL and don't reveal the presence of a coarse mode. On 20 July, 2005 results are shown for two altitudes: 1.5 and 1.8 km. A coarse mode in the retrieved PSD is observed but it is shifted toward smaller radii when compared with sun photometer. The fine mode is stable through the PBL and agrees well with sun photometer. The retrieval of the coarse mode from lidar measurements is a significant issue, because backscattering at 1064 nm wavelength doesn't contain sufficient information about particles of $\sim 5 \mu\text{m}$ size. In our previous paper⁹ we performed simulations trying to understand the possibility to retrieve the coarse mode

with maximum of volume density distribution $\frac{\partial V}{\partial \ln r}$

at $3 \mu\text{m}$ from the present set of wavelengths. For such radii the lidar should reveal the presence of coarse mode although the uncertainty in the input optical data must be less than 10%. In the case considered here, the radii are larger ($5 \mu\text{m}$) so the task is even more difficult. Improvements can be attained with improving of accuracy of input optical data calculation.

4. CONCLUSION

The comparison of aerosol parameters retrieved from multi-wavelength lidar and sun photometer is summarized in Table 1. The lidar provides trustworthy estimation of fine mode parameters such as effective

radius, concentration and complex refractive index. But at the present, the lidar technique has difficulty in retrieving the coarse mode with sufficient accuracy. Improvements in the coarse mode retrieval require input optical data of lower absolute errors.

Table 1. Comparison of aerosol parameters (fine mode) retrieved from lidar and SP on 2 August, 2005

Parameter	Lidar	SP
$r_{\text{eff}}, \mu\text{m}$	0.14 ± 0.1	0.149
$C_v, \mu\text{m}^3/\text{cm}^2$	55 ± 10	75
m_R	1.42 ± 0.05	1.39
m_I	0.005 ± 0.0025	0.0042

REFERENCES

1. D. Müller, A. Ansmann, F. Wagner, D. Althausen, K. Franke. *J.Geophys.Res.*, 107, 4248, doi:10.1029/2001JD001110, (2002).
2. I. Veselovskii, A. Kolgotin, V. Griaznov, D. Müller, U. Wandinger, D. Whiteman. *Appl.Opt.* 41, 3685-3699 (2002).
3. I. Veselovskii, A. Kolgotin, D. Müller, D. N. Whiteman. *Appl. Opt.* 44, 5292-5303 (2005).
4. Dubovik, O., B. N. Holben, T. F. Eck, A. Smirnov, Y. J. Kaufman, M. D. King, D. Tanré, and I. Slutsker, *J. Atmos. Sci.*, 59, 590-608 (2002).
5. Holben, B.N., et al., *Remote Sens. Environ.*, 66, 1-16 (1998).
6. R.A. Ferrare, D. Turner, L. Brasseur, W. Feltz, O. Dubovik, T. Tooman, *J.Geophys.Res.* 106 (D17), 20.333-20.347 (2001).
7. D.S. Balis, V. Amiridis, C. Zerefos, E. Gerasopoulos, M. Andreae, P. Zanis, A. Kazantzidis, S. Kazadzis, A. Papayannis. *Atmospheric Environment* 37, 4529-4538, (2003).
8. D. Muller, I. Mattis, A. Ansmann, B. Wehner, D. Althausen, U. Wandinger, O. Dubovik, *J.Geophys.Res.* 109, D13206, doi:10.1029/2003JD004200 (2004).
9. I. Veselovskii, A. Kolgotin, V. Griaznov, D. Müller, K. Franke, D.N. Whiteman, *Appl.Opt.* 43, 1180-1195 (2004).